available at www.sciencedirect.com

ScienceDirect

journal homepage: www.elsevier.com/locate/aca

Fiber optic lifetime pH sensing based on ruthenium(II) complexes with dicarboxybipyridine

Helena M.R. Gonçalves[a], *César D. Maule*[b,c], *Pedro A.S. Jorge*[c], *Joaquim C.G. Esteves da Silva*[a,*]

[a] *Centro de Investigação em Química (UP), Departamento de Química, Faculdade de Ciências da Universidade do Porto, R. Campo Alegre 687, 4169-007 Porto, Portugal*

[b] *Departamento de Física, Faculdade de Ciências da Universidade do Porto, Portugal*

[c] *Optoelectronics Unit, INESC Porto, R. do Campo Alegre, 687, 4169-007 Porto, Portugal*

ARTICLE INFO

Article history:
Received 21 April 2008
Received in revised form 9 July 2008
Accepted 23 July 2008
Published on line 6 August 2008

Keywords:
Fiber optic
Ruthenium(II) complexes
Fluorescence intensity
Lifetime measurements
pH sensor
Sol–gel technology

ABSTRACT

The complexes of ruthenium(II) with phenanthroline (Phen), diphenylphenanthroline (Ph_2Phen) and with 4,4′-dicarboxy-2,2′-bipyridine acid (Dcbpy) ($[Ru(Phen)_2Dcbpy]Cl_2$ and $[Ru(Ph_2Phen)_2Dcbpy]Cl_2$) were synthesized and the variation of the correspondent fluorescence intensity and lifetime with the pH characterized. Luminescence intensity, emission wavelength and excited state lifetime all show a typical sigmoid variation with pH in the range 3–9, demonstrating the suitability of this complex for luminescence sensing applications. In aqueous solutions (28% ethanol) the complexes $[Ru(Phen)_2Dcbpy]Cl_2$ and $[Ru(Ph_2Phen)_2Dcbpy]Cl_2$ show, respectively, the following properties: apparent pK_a of 3.6 ± 0.4 and 3.7 ± 0.4; lifetimes of the protonated species $0.46 \pm 0.01\,\mu s$ and $0.38 \pm 0.02\,\mu s$ and ionised species $0.598 \pm 0.001\,\mu s$ and $0.61 \pm 0.08\,\mu s$. The $[Ru(Phen)_2Dcbpy]Cl_2$ complex was immobilised in the tip of optical fibers using a hybrid sol–gel procedure based on tetraethoxysilan and phenyltriethoxysilan enabling pH sensitive fiber probes. The immobilised complex shows the following lifetimes: protonated species $1.05 \pm 0.04\,\mu s$ and ionised species $1.16 \pm 0.04\,\mu s$. These characteristics show that these ruthenium(II) complexes are good indicators for pH sensing, either in aqueous solution or immobilised in sol–gel, and are well suited for intensity and/or frequency domain interrogation.

1. Introduction

Determination of the pH has critical importance for a wide range of applications, namely in the medical, environmental and biotechnological fields [1–13]. The most common pH sensors are electrochemical devices (glass electrodes). Although they can be reliable analytical tools in many situations, they are also prone to be affected by electromagnetic interferences [3]. This fragility can be critical in many industrial environments. On the other hand, when combined with optical fibers, optical pH sensors are suitable for remote monitoring in hazardous environments and insensitive to electromagnetic interferences [1,2,7,13]. These advantages of optical pH sensors, along with the fact that these type of sensors can be very small due to their relative simple setup, have led to an increased focus from the scientific community on optical sensing technologies [4,5]. This has resulted in major developments which made possible the availability of some optical pH sensors in the market [4].

* *Corresponding author.*
E-mail address: jcsilva@fc.up.pt (J.C.G. Esteves da Silva).
0003-2670/$ – see front matter © 2008 Elsevier B.V. All rights reserved.
doi:10.1016/j.aca.2008.07.044

Different luminescent and colorimetric indicators are available that can be used to monitor pH based in changes in the luminescent intensity or absorption coefficient [1–13]. However, these two parameters can be affected by any source of optical power drift and demand for the use of complex reference schemes. Furthermore it becomes necessary to use extensive referencing and recalibration procedures to overcome the problems of using luminescence intensity or absorption coefficients to monitor a parameter. Lifetime, on the other hand, provides a self-referenced measurement [14]. By using long-lived metal–organic complexes, measurements can be made at low cost using frequency domain techniques [15,16].

Ruthenium(II) complexes have interesting photochemical and photophysical properties associated with metal-to-ligand charge-transfer (MLCT) excited state, which makes them good candidates as sensitive receptors for optical sensing applications. Complexes with α-diimine ligands (1,10-phenanthroline, Phen, and 4,7-diphenyl-1,10-phenanthroline, Ph_2Phen), for example, have been widely studied for their unique photophysical properties [16]. Their high quantum yields and their relatively long lifetime in the order of microseconds make them highly suitable for frequency domain luminescence sensing [15]. As such the possibility of creating these kinds of complexes sensitive to pH became a very attractive idea. A strategy to make a polypyridyl luminescent complex with this characteristics includes the use of ligands with ionisable functional groups, for example a carboxylic group (dicarboxy-2,2′-bipyridine acid, Dcbpy) [15,16]. In order to apply these luminescent complexes into an optical fiber probe it is necessary to immobilise them in a suitable solid membrane [17,18]. Ideally these membranes should allow the exchange of protons and provide an effective encapsulation of the complex at the same time that preserves all its sensing properties [3].

Ruthenium complexes $[Ru(Phen)_2Dcbpy]Cl_2$ and $[Ru(Ph_2Phen)_2Dcbpy]Cl_2$ were synthesized, immobilised in a sol–gel matrix and incorporated as sensors in fluorescent optical systems sensitive to pH. The sol–gel technology is a simple route to manufacture porous glass [19,20] with the advantage that the physical characteristics can be tailored by the preparative conditions [21,22]. In addition, the optical properties of these materials, as well as their good adhesion to silica surfaces, make them an excellent choice for optical fiber-based applications. The results obtained regarding the characterization of the steady state and lifetime properties of the synthesized complexes in solution and in sol–gel will be presented and the sensor performance assessed.

2. Experimental

2.1. Reagents

Ruthenium(III) chloride (45–55%), Phen (99.5%), 4,7-diphenyl-1,10-phenanthroline (Ph_2Phen) (97%), lithium chloride (99.5 + %), 4,4′-dicarboxy-2,2′-bipyridine acid (Dcbpy), $C_{12}H_8N_2O_4$ (90%), TEOS (tetraethoxysilane) (≥99%), octyl-triEOS (octytriethoxysilane), (≥96%), tetramethyl orthosilicate (TMOS), phenyltriethoxysilane (Ph-TriEOS) and Triton X-100 were obtained from Sigma–Aldrich Química S.A. (Spain). *N*,*N*-Dimethylformamide (DMF), disodium hydrogenphosphate, potassium dihydrogenphosphate, sodium hydroxide and hydrogen chloride pro-analysis were purchased from Merck, Darmstadt (Germany). Deionised water with resistivity higher than 4 MΩ/cm was used.

2.2. Synthesis of the sensors

2.2.1. Synthesis of $cis[Ru(Phen)_2]Cl_2$ and $cis[Ru(Ph_2Phen)_2]Cl_2$

cis-Dichlorobis(phenanthroline)ruthenium was prepared via a modified literature method [23]. Ruthenium(III) chloride (1.61 g) and 1,10-phenanthroline (2.45 g) were refluxed in 60 mL of DMF for 3 h. Most of the solvent was then distilled off and the remaining solution was cooled to room temperature, treated with acetone (50 mL) and kept overnight at 0 °C. The crystals formed were collected by suction filtration and washed with water. The crude product was suspended in 140 mL of water/ethanol (1:1) and heated to reflux for 1 h. The solid was filtered and treated carefully with lithium chloride (30 g). Ethanol was distilled off and the resulting water solution was cooled in an ice bath resulting in the precipitation of dark crystals. The only difference for *cis*-dichlorobis(diphenylphenanthroline)ruthenium was the addition of 0.6476 g of 4,7-diphenyl-1,10-phenanthroline.

2.2.2. Synthesis of $[Ru(Phen)_2Dcbpy]Cl_2$ and $[Ru(Ph_2Phen)_2Dcbpy]Cl_2$

$[Ru(Phen)_2Dcbpy]Cl_2$ and $[Ru(Ph_2Phen)_2Dcbpy]Cl_2$ were prepared via a modified literature method [16]. Dcbpy was reacted with *cis*-dichlorobis(phenanthroline)ruthenium or *cis*-dichlorobis(phenylphenanthroline)ruthenium (1:1) in a mixture of methanol/water (4:1) under an nitrogen atmosphere. The reaction mixture was refluxed for approximately 16–24 h and at the end it was reduced to a third of its original volume. The complex $[Ru(Ph_2Phen)_2Dcbpy]Cl_2$ was precipitated with a saturated solution of sodium chloride and the solid was extracted with methanol. The complex $[Ru(Phen)_2Dcbpy]Cl_2$ was precipitated with ether/acetone (3:1, v/v) and the solid was dissolved in methanol. The complexes precipitated standing overnight at 0 °C.

2.3. Acid–base titrations

Saturated aqueous solutions of the two ruthenium(II) complexes were prepared in water/ethanol (1:1). Six-hundred microliters of the saturated solution was added to 850 μL of phosphate buffer with pH adjusted in the range from 2 to 9 and 150 mL of ethanol—the final ethanol percentage was 28%. All solutions under analysis were air equilibrated to obtain a constant concentration of oxygen.

2.4. Immobilisation on sol–gel matrices

2.4.1. Sol–gel with TEOS, octyl-triEOS and Triton-X

Two-hundred microliters of TEOS, 10 μL of octyl-triEOS, 124.8 μL of ethanol, 20 μL of 0.1 M hydrogen chloride and 30 μL of Triton-X were added and mixed for 45 min [24]. Afterwards 100 μL of a saturated solution of the complex in water/ethanol

(1:1) was added to the sol–gel and shaken for 10 min. Thin films were made by dip-coating.

2.4.2. *Sol–gel with TMOS*

Equal amounts of TMOS and hydrogen chloride (pH 3) were added and mixed for 2 h at room temperature [2]. The resulting solution became a clear and homogeneous sol–gel. An equal volume from a saturated solution of the complexes in water/ethanol (1:1) was added to the sol–gel and thin films were made by dip-coating.

2.4.3. *Sol–gel with TEOS and Ph-TriEOS*

This sol–gel matrix was prepared based on a literature method [18] and consisted in the following: 1 mL of TMOS and 25 μL Ph-TriEOS were mixed with 0.4 mL of hydrogen chloride 0.1 M and 1.15 mL of a saturated solution of the complex in water/ethanol (1:1). The mixture was shaken for 20 min before films were immobilised in glass plates and optical fibers by dip-coating.

2.4.4. *Preparation of optical fiber probes*

Silica optical fibers with core/cladding diameters of, respectively, 550 and 600 μm were purchased from Thorlabs. The fiber tips were carefully polished and their protective coating removed with acetone followed by rinsing with deionised water. To enhance the efficiencies of excitation and collection of luminescence the fiber tips were reshaped by chemical etching. By slow and controlled immersion of the tip in 40% HF a tapered probe with conical shape was obtained (in a 2-cm fiber length the diameter is reduced from 600 to approximately 200 μm). To obtain the luminescent probes the fibers were then dip-coated with the dye-doped sol–gel solutions and left to dry in a clean environment at ambient temperature.

2.5. *Instrumental setup*

A Spex 3D Spectrofluorimeter with a 75-W xenon lamp and a CCD detector was used. EEM were acquired, in an excitation wavelength range from 200 to 675 nm, and in an emission wavelength range from 201 to 720 nm, with a resolution of 5 nm.

Lifetime data for luminescent fiber probes was acquired at room temperature using frequency domain interrogation. A blue laser diode (473 nm) was used as the excitation source. The laser output could be sinusoidally modulated in the 1–10 MHz frequency range. The luminescence emission was guided to the probe by a 600-μm Y fiber coupler. Luminescence was collected by the same optical fiber and lead to detection by a variable gain amplified silicon photodetector (PDA36A from Thorlabs, Inc.) set at 30 dB amplification and 785 kHz bandwidth. The signal obtained by the detector was fed into a lock-in amplifier (SR844 from SRS) where it was compared with a reference signal from the modulation source. By this method the relative phase difference was obtained. Under these conditions, the luminescence emission is also a sinusoidal signal, with the same modulation frequency (f) but having a phase shift proportional to the lifetime of the excited state (τ).

The lifetime data of sample solutions was obtained using a similar set-up. In this case a UV LED (350 mcd, 400 nm) was used to excite the sample by direct irradiation. Luminescence signals were then collected at 90° by the fiber system.

2.6. *Data analysis*

The variations in the fluorescence intensity of the complexes resulting from the deprotonation/protonation reaction of the ligand Dcbpy (monoprotic acid) can be linearized using a Henderson–Hasselbalch type equation (Eq. (1)) which allows the calculation of the pK_a for each complex [25]:

$$\mathrm{pH} = \mathrm{p}K_\mathrm{a} + \log\left[\frac{I_\mathrm{max} - I}{I - I_\mathrm{min}}\right] \quad (1)$$

where I_max and I_min are, respectively, the maximum and minimum of the fluorescence intensity of the acid or conjugated base species and I is the fluorescence intensity as function of the pH.

The lifetime of the excited state of the complex (either protonated and deprotonated) (τ) can be calculated using frequency domain spectroscopy [26]. Typically the sinusoidal modulation is applied in frequencies that are within the range of the reciprocal of the excited state lifetime. When the luminescent complex is excited with a sinusoidally modulated source a luminescent signal with sinusoidal modulation can de detected. However, due to the finite lifetime of the complex the luminescent signal is delayed relative to the excitation signal. The time delay can be measured as a phase shift, ϕ, that depends on the modulation frequency, f. These parameters can be related by Eq. (2) allowing an estimation of the lifetime:

$$\tan(\phi) = 2\pi f\tau \quad (2)$$

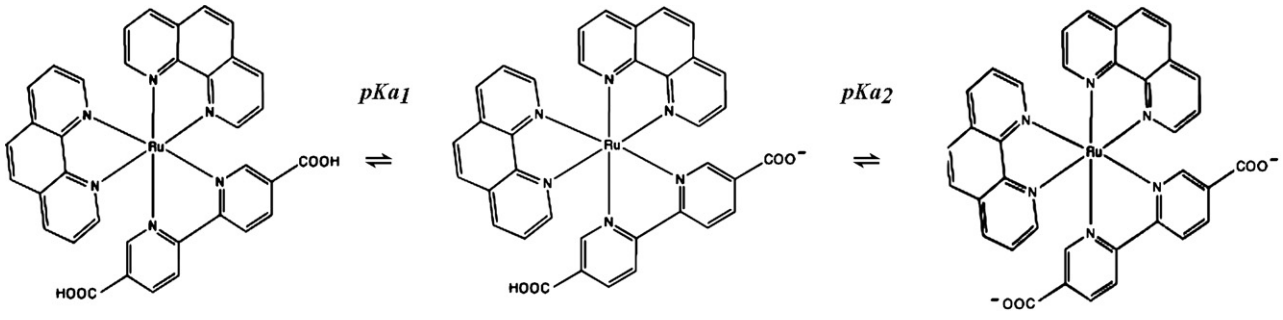

Fig. 1 – Schematic representation of the protonation–deprotonation equilibrium for the $[Ru(phen)_2Dcbpy]Cl_2$ (Ru_A) complex.

3. Results and discussion

3.1. *Effect of the pH on the emission spectra*

To facilitate discussion, from this point forward, the complexes $[Ru(Phen)_2Dcbpy]Cl_2$ and $[Ru(Ph_2Phen)_2Dcbpy]Cl_2$ will be addressed, respectively, as Ru_A and Ru_B. As an example, the chemical structure of Ru_A and the corresponding protonation–deprotonation equilibria are shown in Fig. 1. In addition, the excitation and emission spectra of the protonated and deprotonated forms for complexes Ru_A and Ru_B are presented in Fig. 2 and a summary of their properties is presented in Table 1. The results obtained clearly show that the emission band is pH sensitive suffering a red shift upon ionisation and presenting also a relatively large Stokes shift of about 200 nm. Both these features are an added value from the point of view of an optical fiber sensor configuration. The large Stokes shift facilitates discrimination between the excitation radiation and the luminescent signal, reducing the need for filtering. On the other hand, the red shift provides a mechanism to measure pH based on wavelength, which is an absolute parameter, and also allows for a more sensitive detection as the photodetector responsivity increases towards the infrared. Moreover, both the protonated and deprotonated forms of the complexes are strongly fluorescent. Overall these properties make these complexes adequate for fluorescence pH sensing. Moreover, both the protonated and deprotonated forms of the complexes are strongly fluorescent which make them adequate for fluorescence pH sensing.

A detail analysis of the emission intensity spectrum variation with the pH was done and a marked increase of the emission fluorescence was observed when the pH was increased in the range from 2.0 up to 4.5. Fig. 3a shows, as an example, the data obtained for the Ru_A complex. It can be observed that there is a difference between the emission characteristics of the protonated and deprotonated complex. In addition to the change in intensity, an apparent shift in the emission peak to shorter wavelengths takes place as pH increases. The absorption of light (near 450 nm) by the complexes results in a metal-to-ligand charge transfer (MLCT) transition [26]. The emission from the MLCT state is the relatively long lifetime fluorescence—in the order of microseconds. The results obtained in this work suggests that the deprotonated form of the Dcbpy ligand is probably a better electron acceptor than the protonated form; the deprotonated Dcbpy increases the MLCT state, shifting the emission to shorter wavelengths as the pH is increased. This behaviour is interesting from the application point of view as it enables the use of ratiometric schemes. Similar results were obtained for complex Ru_B.

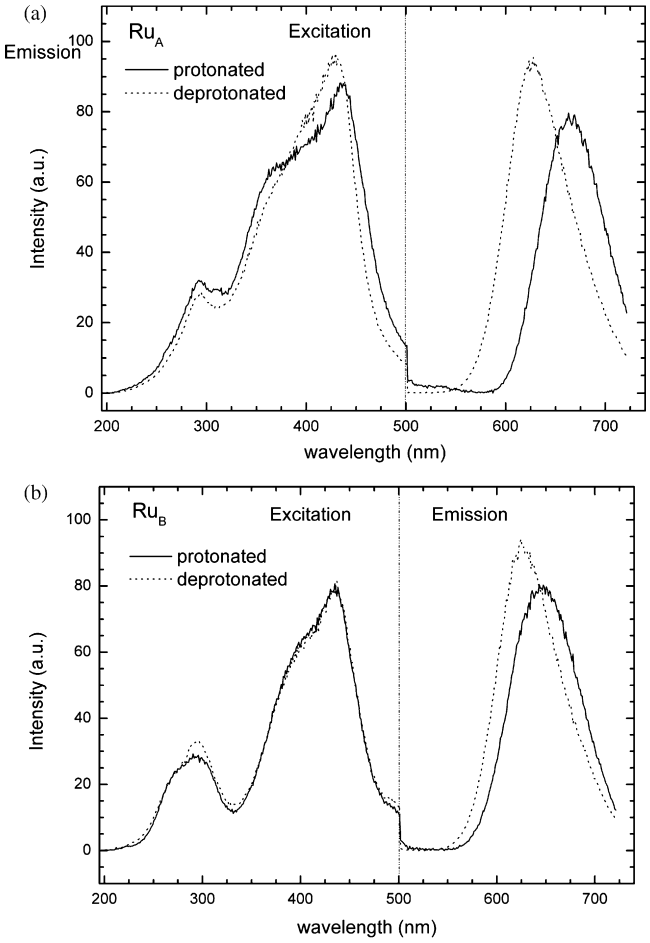

Fig. 2 – Excitation and emission spectra of the $[Ru(phen)_2Dcbpy]Cl_2$ (Ru_A) (a) and $[Ru(Ph_2phen)_2Dcbpy]Cl_2$ (Ru_B) (b) complexes in water/ethanol (1:1): (···) protonated and (—) ionised species.

Table 1 – Acid–base and photophysical properties of the synthesised complexes

Property	Complex	
	$[Ru(Phen)_2Dcbpy]Cl_2$	$[Ru(Ph_2Phen)_2Dcbpy]Cl_2$
Excitation wavelength (nm)	431	435
Emission wavelength of the protonated complex (nm)	628	625
Emission wavelength of the ionised complex (nm)	665	640
Emission wavelength of the sol–gel immobilised complex (nm)	628	
pK_a	3.6 ± 0.4	3.7 ± 0.4
Lifetime of the protonated complex (μs)	0.46 ± 0.01	0.38 ± 0.02
Lifetime of the ionised complex (μs)	0.598 ± 0.001	0.61 ± 0.08
Lifetime of the sol–gel immobilised protonated complex (μs)	1.05 ± 0.04	
Lifetime of the sol–gel immobilised ionised complex (μs)	1.16 ± 0.04	

*These values represent an average value obtained from at least three independent measurements.

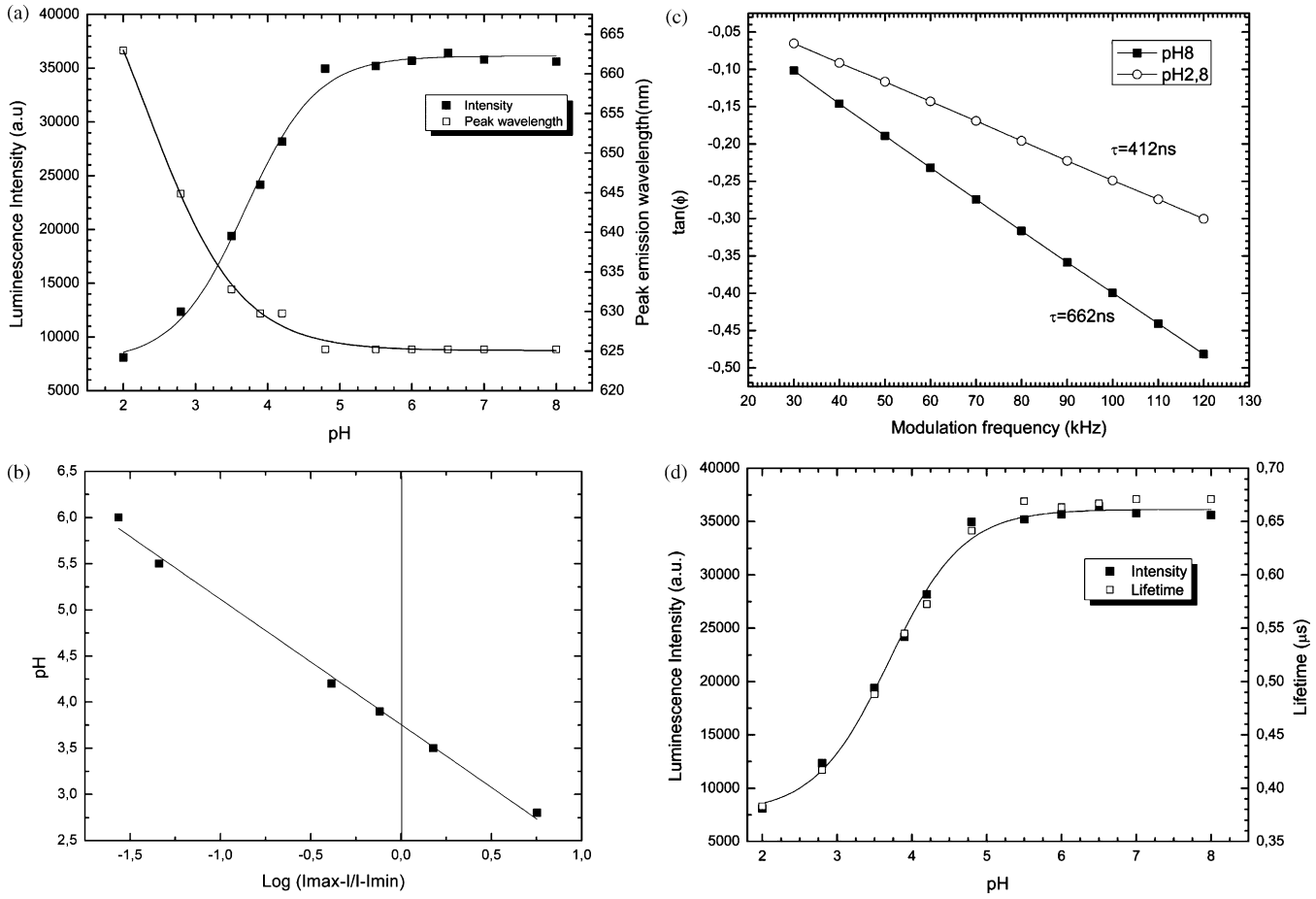

Fig. 3 – Fluorescence intensity and peak emission wavelength as function of pH (a), Henderson–Hasselbalch plot of the intensity variation as function of the pH (b), phase as function of the modulation frequency in pH buffer 2.8 (●) and 9.0 (○) (c) and lifetime change with pH (d) of [Ru(phen)$_2$Dcbpy]Cl$_2$ (Ru$_A$).

The fluorescence intensity variation with pH presented in Fig. 3a represents a well-shaped sigmoidal titration curve with one inflection point which is compatible with a monoprotic acid and, consequently, the curve can be linearized by fitting the experimental data to a Henderson–Hasselbalch model as shown in Fig. 3b (Eq. (1)). From this plot a pK_a of about 3.6 can be estimated (Table 1). The pK_a found for both complexes are very similar with a literature reported value (3.19 ± 0.04 [16]) and the difference may be attributed to the different ethanol percentages used in both works.

3.2. *Effect of the pH on the lifetime*

The excited state lifetimes of both complexes (protonated and deprotonated forms) were calculated from the plot of the phase ($\tan\phi$) as a function of the modulation frequency (Eq. (2)) (Fig. 3c) shows, as an example, data obtained for complex Ru$_A$ (Table 1). Using the same method, the lifetime of the two complexes as function of the pH was calculated and a typical curve is shown in Fig. 3d (this curve is overlaid with the curve of the intensity variation with the pH).

The analysis of the lifetimes of both complexes (Table 1 and Fig. 3d) shows that the protonated species have a lifetime of about 0.4 μs and the ionised species have a lifetime of about 0.6 μs, which means that lifetime not only changes with the solution pH but it has a similar trend, *i.e.*, the lifetime increases as the solution pH increases. This result agrees with the energy-gap law that states that the non-radiative decay rate increases exponentially as the emission energy decreases [26]. Indeed, as discussed above, the deprotonation of Dcbpy shifts the emission to shorter wavelengths (higher energies) and, supporting the band-gap theory, the lifetime also increases. The lifetime values found in this work are in the same range as others described in the literature a well as the increasing lifetime trend as the complex is ionised [16]. The range of lifetime variation upon ionisation is well suited for frequency domain interrogation.

The analysis of Fig. 3d shows that the lifetime of both complexes has a sigmoid type variation, very similar to that of the intensity. This indicates that the intensity quenching/enhancement mechanisms are directly coupled to the increase/decrease of non-radiative decay pathways. This result is quite relevant in terms of the analytical chemistry importance of these complexes for lifetime-based pH sensors since this variation can easily be linearized using a Henderson–Hasselbalch type model (Eq. (1)) showing that it can be used to effectively measure the solution pH.

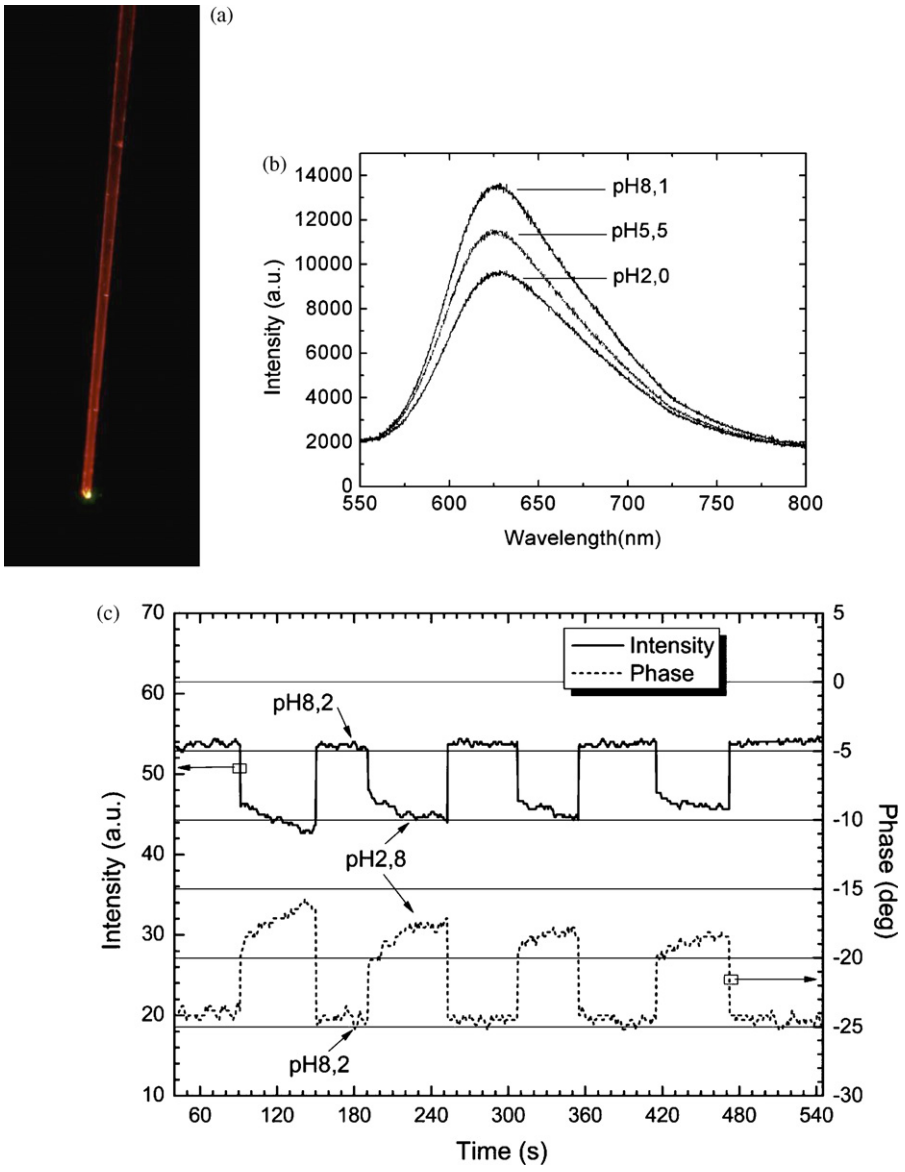

Fig. 4 – Photograph of the tip of the fluorescence fiber probe (a) and emission spectra as function of the pH of the $[Ru(Phen)_2Dcbpy]Cl_2$ (Ru_A) complex immobilised at the tip of the optical fiber (b). Phase and intensity response cycles (integration of the fluorescence intensity between 600 and 660 nm) to pH 2.8 and 8.1 of the complex $[Ru(Phen)_2Dcbpy]Cl_2$ (Ru_A) immobilised in the tip of an optical fiber—phase and intensity at 150 kHz measured from lock-in amplifier (c).

3.3. *Complexes immobilised on sol–gel matrices*

The three sol–gel preparations were successful in the immobilization of the Ru(II) complexes and no leaching was observed. Also, when in contact with water, the sol–gel structures (membranes or monoliths) were mechanically stable. The matrixes are described by timeframe, when it was found that the sol–gel did not corresponded to the objective intended it was changed by another one.

With the TEOS/octyl-triEOS-based sol–gel membrane it was possible to make a thin and robust film that was stable when in contact with different pH solutions and the lifetime of the immobilised Ru_A complex was about 1.09 μs. However, when immersed in aqueous solutions the Ru(II) complexes immobilised in the sol–gel membrane demonstrated a slow response to the solution pH (≈30 min). This matrix was therefore abandoned and another one was tested.

The TMOS-based sol–gel membrane successfully entrapped the Ru_A complex and the lifetime of the complex inside the dry matrix was about 0.58 μs. However, when in contact with different pH buffers, it was not possible to measure any change in lifetime.

Best results were obtained, with a TEOS/Ph-triEOS-based sol–gel membrane where it was observed a measurable and rapid variation (30 s) of the luminescence emitted by the immobilised complex when in contact with aqueous solutions at different pH (Fig. 4). Consequently, this sol–gel was used to immobilise the complex on the tip of optical fibers and its performance was characterized.

3.4. *Complexes coupled to optical fibers*

Fig. 4a shows a picture of the luminescent fiber probe (image taken through a long pass filter with cut-off at 550 nm), the corresponding emission spectra as function of the pH (Fig. 4b) and the dynamic response of fluorescence intensity and phase to cycles between two different pH buffers (2.8 and 8.1) (Fig. 4c). These results show that the intensity and lifetime behaviour of the immobilised complex are a function of the pH when the tip of the optical fiber is immersed in aqueous solution with different acidity and that the responses are quite reproducible. The analysis of Fig. 4c shows that the response time of the full ionisation is less than 1 min and the reverse is a much faster process taking less than 10 s. Fig. 4b shows that decreasing the pH provokes a proportional decrease of the fluorescence intensity and, contrary to previously observed in aqueous solution (Fig. 3a), no measurable wavelength shift is observed. While in solution the intensity was decreased by almost 80% when going from alkaline to acid environment. After immobilization the quenching observed in the same situation is of approximately 30%. This indicates that a given population of immobilised dye is not ionisable remaining in the acidic state. In addition, rigidochromism effects are known to cause a blue shift in the emission of immobilised dyes. As a result, the overall emission of the luminescent fiber probes shows a maximum of the emission spectra of the immobilised complex at about 628 nm (Table 1).

In spite of all, it is still feasible to perform pH measurements using either the luminescence intensity or the lifetime response of the fiber probes. Fig. 5 shows the variation of the lifetime and fluorescence intensity of the immobilised Ru_A in sol–gel (TEOS + Ph-TriEOS). The analysis of Fig. 5a shows that the lifetime response of the immobilised complex can still be fitted by a sigmoid (similar result was observed for the fluorescence intensity) as function of the pH. The behaviour is similar to that observed in aqueous solution, with an ionisation constant in the same range. After the immobilization, however, the sigmoidal curve is much broader than in solution. This may be due to different microenvironments in the solid matrix having different sensitivity to pH, therefore having different pK_a. This pK_a distribution then results in a response over a broader pH range.

The analysis of the lifetimes of the immobilised Ru_A complex in sol–gel (TEOS + Ph-TriEOS) (Table 1) shows that the protonated species have a lifetime of $1.05 \pm 0.04\,\mu s$ and the ionised species have a lifetime of $1.16 \pm 0.04\,\mu s$, showing a similar trend as that observed in aqueous solution—the lifetime increases as the solution pH increases. However, the immobilised complex shows a lifetime nearly double than in aqueous solution. In addition, the relative change in lifetime is smaller than in solution. These results confirm the existence of a population of immobilised dye that is not responsive to pH. This decreased sensitivity may also be related to the fact that the sol–gel matrix was prepared in an acidic media, where the luminescence intensity is lowest. Nevertheless the behaviour observed in the solid matrix when compared to the one in solution (see Fig. 5b) shows that the intensity and lifetime of the immobilised complex respond reversibly and reproducibly to the pH of the aqueous solution. Careful observation shows that although the sensor

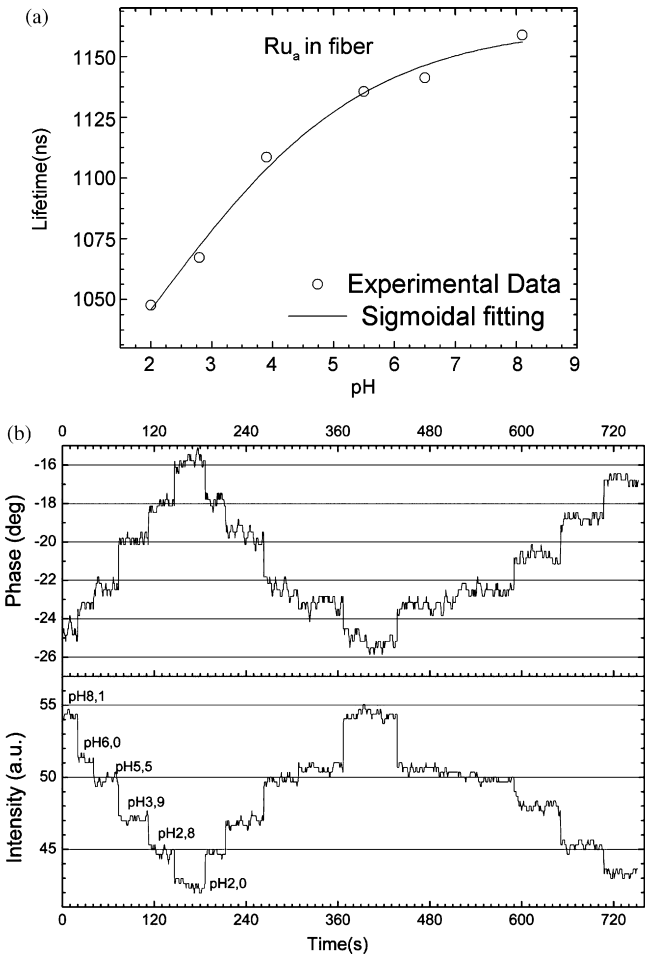

Fig. 5 – Lifetime dependence with pH of the immobilised $[Ru(Phen)_2Dcbpy]Cl_2$ (Ru_A) in sol–gel (TEOS + Ph-TriEOS) (a) and the dynamic response of lifetime and intensity to a sequence of increasing/decreasing pH values (b).

response is quite stable in alkaline environments in very acidic media some drift is observed. This is mainly the result of the reduced luminescence intensity at low pH reducing the system signal-to-noise ratio. Further optimization of the sol–gel processing parameters should allow the improvement of these parameters by increasing the amount of dye available for ionisation.

The long-term operation of the sensors was not tested in a systematic fashion; nevertheless, it could be observed that the sensor was stable over several test sessions of some hours, showing a strong luminescent output. To minimize drift effects due to slow photobleaching, however, calibration should be performed at the beginning of each probing session. In addition, it was observed that fiber probes stored in the dark were still operational after more than 2 months.

The main expected interferences to the sensors are the temperature and the percentage of oxygen dissolved in the solution under analysis. Under laboratory conditions these two factors are easily controlled but for field measurements the dissolved oxygen and the temperature should be monitored. To check, in particular, the influence of dissolved oxygen on the sensor performance, the phase output was recorded

while the sensor was immersed in a container of deionized water which was successively bubbled with nitrogen and compressed air. This procedure allowed submitting the sensor to cycles of dissolved oxygen concentration from 9 to 0 mg/L. In this interval it was observed that a phase change of 1° was induced in the sensor. The magnitude of this phase change is comparable to the one induced by a change of 1 pH unit (~1.5°). Nevertheless, in most applications fluctuations on oxygen concentration are likely to be much smaller, greatly reducing the induced error. In any case, simultaneous measurement of the pH and the interfering parameters is possible. In fact, this could be done in an all-optical system as fiber optic sensors for temperature and oxygen have been developed, using similar instrumentation, that can be easily coupled to the fiber optic pH sensor presented here [27–32].

These results demonstrate that the synthesized complexes are suitable for optical sensing and when compared to other pH sensors previously described in the literature both sensors and immobilization matrix represents an improvement in some parameters. For example, the pH sensor described in Ref. [33] is based on immobilised fluoresceinamine. This fluorophore is well known and is highly luminescent, however, when immobilised in cellulose, the intensity response above pH 8 decreases due to the hydrolysis of the sensor which means that it only work in a pH range between 3 and 8. Furthermore, the background noise, due to the fact that the maximum emission wavelength and the excitation are less than 60 nm apart, is 40% of the signal at pH 3 and decreases with increasing pH, which makes the measurements for pH 3 up to 5 difficult. Another optical sensing pH sensor is based on Congo Red immobilised in a cellulose acetate film [34]. This sensor has an intensity response less affected by background noise, as the complex described in our work, however, the response in solution is completely different when compared to the behaviour in solid matrix and this difference is not yet completely understood. Moreover the film response changed about 3% over a 6-h period of measurement which maybe due to leaching problems. In this context, the fact that the proposed sensor is based in lifetime interrogation allows to overcome some limitations due to optical power drift and signal fading due to leaching.

4. Conclusion

The complexes $[Ru(Phen)_2Dcbpy]Cl_2$ and $[Ru(Ph_2Phen)_2 Dcbpy]Cl_2$ are pH sensitive luminescent indicators, suitable to be incorporated in optoelectronic systems. Their lifetime in the microsecond range enables the implementation of frequency domain interrogation with relatively low modulation frequencies allowing for low cost instrumentation. In addition, the large Stokes shift and high quantum yield facilitate photodetection. Both complexes have a pK_a of about 3.6. These complexes have a lifetime in the order of hundreds of nanoseconds and a measurable change in lifetime upon ionisation. Both complexes can be successfully immobilised in different sol–gel matrices and a hybrid sol–gel (*TEOS and Ph-TriEOS*) allows an adequate pH response (intensity and lifetime) for the immobilised complex. The fiber optic pH sensor developed and assessed is easily assembled using general laboratory reagents and quite simple experimental procedures.

Acknowledgements

Financial support from Fundação para a Ciência e Tecnologia (Lisboa) (FSE-FEDER) (Projects PTDC/QUI/71001/2006 and POCTI/QUI/44614/2002) is acknowledged. César Maule acknowledges the support from the Marie Curie Early stage research training network, funded by European Commission under the contract MEST-CT-2005-020353.

REFERENCES

[1] A. Dybko, W. Wroblewski, E. Rozniecka, K. Poznisk, J. Maciejewski, R. Romaniuk, Z. Brozozka, Sens. Actuators B: Chem. 51 (1998) 208.
[2] C. Malins, H.G. Glever, T.E. Keyes, J.G. Vos, W.J. Dressick, B.D. MacCraith, Sens. Actuators B: Chem. 67 (2000) 89.
[3] P.A.S. Jorge, P. Caldas, J.C.G. Esteves da Silva, C.C. Rosa, A.G. Oliva, F. Farahi, J.L. Santos, Fiber Integr. Optics 24 (2005) 201.
[4] B.R. Swindlehurst, R. Narayanaswamy, Optical sensing of pH in low ionic strength waters, in: R. Narayanaswamy, O.S. Wolbeis (Eds.), Optical Sensors—Industrial Environmental and Diagnostic Applications, Springer, New York, 2004, pp. 281–308 (Chapter 12).
[5] G. Orellana, D. Garcia-Fresnadillo, Environmental and industrial optosensing with tailored luminescent Ru(II) polypyridyl complexes in optical sensors, in: R. Narayanaswamy, O.S. Wolbeis (Eds.), Optical Sensors—Industrial Environmental and Diagnostic Applications, Springer, New York, 2004, p. 309 (Chapter 13).
[6] M. Fritzsche, C.G. Barreiro, B. Hitzmann, T. Scheper, Sens. Actuators B: Chem. 128 (2007) 133.
[7] P.C.A. Jerónimo, A.N. Araújo, M.C.B.S.M. Montenegro, Talanta 72 (2007) 13.
[8] M.P. Seidel, M.D. DeGrandpre, A.G. Dickson, Mar. Chem. 109 (2008) 18.
[9] L. Brigo, T. Carofiglio, C. Fregonese, F. Meneguzzi, G. Mistura, M. Natali, U. Tonellato, Sens. Actuators B: Chem. 130 (1998) 477.
[10] F.Y. Ge, L.G. Chen, J. Fluoresc. 18 (2008) 741.
[11] A. Hakonen, S. Hulth, Anal. Chim. Acta 606 (2008) 63.
[12] M. Bradley, L. Alexander, K. Duncan, M. Chennaoui, A.C. Jones, R.M.S. Martin, Bioorg. Med. Chem. Lett. 18 (2008) 313.
[13] S. Dong, M. Luo, G. Peng, W. Cheng, Sens. Actuators B: Chem. 129 (2008) 94.
[14] U. Kosch, I. Klimant, T. Werner, O. Wolfbeis, Anal. Chem. 70 (1998) 3892.
[15] J. Lin, C.W. Brown, Trends Anal. Chem. 19 (2000) 541.
[16] Y. Clarke, W. Xu, J.N. Demas, B.A. DeGraff, Anal. Chem. 72 (2000) 3468.
[17] Y. Amao, Microchim. Acta 143 (2003) 1.
[18] E. Wang, K.F. Chow, V. Kwan, T. Chin, C. Wong, A. Bocarsly, Anal. Chim. Acta 495 (2003) 45.
[19] J.M. Price, W. Xu, J.N. Demas, B.A. DeGraff, Anal. Chem. 70 (1998) 265.
[20] J. Lin, C.W. Brown, Trends Anal. Chem. 16 (1997) 200.
[21] C.J. Brinker, G.W. Scherer, Sol–gel Science, Academic Press, New York, 1990.
[22] C.J. Brinker, J. Non-Cryst. Solids 100 (1988) 31.
[23] G. Sprintschnik, H.W. Sprintschnik, P.P. Kirsch, D.G. Whitten, J. Am. Chem. Soc. (1977) 4947.

[24] T.S. Yeh, C.S. Chu, Y.L. Lo, Sens. Actuators B: Chem. 119 (2006) 701.
[25] D.A. Skoog, D.M. West, F.J. Holler, Fundamentals of Analytical Chemistry, 7th ed., Saunders College Publishing, Fort Worth, 1996.
[26] J.R. Lakowicz, Principles of Fluorescence Spectroscopy, 2nd ed., Kluwer–Plenum, New York, 1999.
[27] A.K. McEnvoy, C.M. McDonagh, B.D. MacCraith, Analyst 121 (1996) 785.
[28] P.A.S. Jorge, P. Caldas, C.C. Rosa, A.G. Oliva, J.L. Santos, Sens. Actuators B: Chem. 103 (2004) 290.
[29] O.S. Wolfbeis, Anal. Chem. 78 (2006) 3859.
[30] S.M. Borisov, A.S. Vasylevska, C. Krause, O.S. Wolfbeis, Adv. Funct. Mater. 16 (2006) 1536.
[31] P.A.S. Jorge, C. Maule, A.J. Silva, R. Benrashid, J.L. Santos, F. Farahi, Anal. Chim. Acta 606 (2008) 223.
[32] Y.L. Lo, C.S. Chu, J.P. Yur, Y.C. Chang, Sens. Actuators B: Chem. 131 (2008) 479.
[33] L.A. Saari, W.R. Seitz, Anal. Chem. 54 (1982) 821.
[34] T.P. Jones, M.D. Porter, Anal. Chem. 60 (1988) 404.